X-693-75-258
PREPRINT

IMPLICATIONS OF PIONEER-II MAGNETIC FIELD MODELS FOR JUPITER'S DECAMETRIC RADIO MISSION

J. K. ALEXANDER
R. A. SMITH
M. L. KAISER
M. H. ACUNA
R. F. THOMPSON

OCTOBER 1975

GSFC — GODDARD SPACE FLIGHT CENTER —
GREENBELT, MARYLAND

Implications of Pioneer-11 Magnetic Field Models for Jupiter's Decametric Radio Emission

J.K. Alexander, R.A. Smith, M.L. Kaiser,
M.H. Acuna and R.F. Thompson

Prepared for presentation at meeting
of USNC/URSI,
Boulder, Colorado (October, 1975)

IMPLICATIONS OF PIONEER-11 MAGNETIC FIELD MODELS FOR JUPITER'S DECAMETRIC RADIO EMISSION

J.K. Alexander, R.A. Smith, M.L. Kaiser
M.H. Acuna and R.F. Thompson
Laboratory for Extraterrestrial Physics
Goddard Space Flight Center
Greenbelt, Maryland

ABSTRACT

Models of Jupiter's magnetic field derived from measurements with the Pioneer-11 flux gate and vector helium magnetometers have been analyzed with a view towards understanding the origin of the decameter-wave radio emission (DAM) from the planet. In particular, we have calculated the geometry and electron gyrofrequency predicted for both the North and South feet of the Io-threaded flux tube at several altitudes as a function of sub-Io longitude for the multipole field models of Acuña and Ness (1975) and Smith et al. (1975). The models predict a maximum surface gyrofrequency equal to the observed high frequency limit of the DAM and tend to favor a mechanism involving transverse propagation from a source in the Northern hemisphere. Although a detailed understanding of the DAM cannot be derived from either model, our calculations indicate that the beaming pattern of the emission may be determined by reflection from the ionosphere rather than by inherent beaming from the source region.

I. Introduction

The first in situ measurements of fields and particles in the Jovian magnetosphere by instruments on Pioneer 10 (closest approach = 2.85 R_J) provided a valuable new body of information regarding the magneto-ionic environment of the planet. However, our insight into the nature and origin of Jupiter's decameter-wave radio emission (DAM) did not enjoy commensurate advances as a result of new findings from the spacecraft experiments. The radio astronomical predictions concerning the sign, gross orientation, and dipole moment of the Jovian magnetic field were verified, but more detailed models of the magnetic field derived from the Pioneer data did not lead to explanations of the morphological characteristics of DAM. For example, Smith and Wu (1974) showed that the variation of electron gyrofrequency at the feet of the Io-threaded flux tube (IFT) with rotation of the planet did not show any clear correspondence to the gross frequency structure observed in dynamic spectra of the Io-controlled DAM emissions.

With the closer and retrograde encounter of Jupiter by Pioneer 11 (1.7 R_J) it became possible to improve the models of the magnetic field. We have used those updated models as derived from the vector helium magnetometer on Pioneer 10 and 11 (Smith, et al., 1975) and the fluxgate magnetometer on Pioneer 11 (Acuña and Ness, 1975) in order to take a further look at the implications of our present view of the magnetic field for understanding DAM.

The magnetic field model of Smith et al. (1975) is a 23-coefficient spherical harmonic expansion having dipole, quadrupole, and octupole terms for internal sources and first and second order terms for external sources. The O_4 model of Acuña and Ness (1975) uses only internal terms up through octupole order. We have adopted the working hypothesis that the IFT is the important source region to investigate, and we have begun our analysis with computations of the zenographic location and vector magnetic field of the IFT as a function of System III (1965)* sub-Io longitude.

II. The Io Fluxtube Motion

In Figure 1 we have plotted the surface electron gyrofrequency at the North and South foot points of the IFT and the magnetic dip angle at 5.91 R_J (Io's orbital distance) at the zenographic equator as a function of System III (1965) sub-Io longitude. Representative plots of DAM occurrence probability vs. sub-Io longitude for the four Io controlled "sources" are also shown for comparison. As was noted by Smith and Wu (1974), the maximum value of the gyrofrequency at the North foot of the IFT is essentially identical to the maximum observed emission frequency of 39.5 MHz for DAM. Since the gyrofrequency at the South foot point never exceeds 28 MHz, the North foot of the IFT would appear to be more attractive as the source for the three high-

*The new System III (1965) longitude convention (Riddle, 1975) gives System III longitudes $\simeq 30^{\circ}$ lower than System III (1957.0) for observations at the time of Pioneer-11 encounter.

frequency Io-controlled sources. A problem still exists in that the sub-Io longitude of the early source (which reaches the highest emission frequency) does not correspond to the region of maximum gyrofrequency at the IFT foot point. Interestingly, the maximum gyrofrequency in the Southern hemisphere (28 MHz) is the same as the highest frequency at which Io-independent DAM is observed. This is the maximum gyrofrequency for trapped electrons since their minimum mirror altitudes will be determined by the weaker Southern magnetic field. On the other hand, precipitating electrons in the Northern hemisphere could account for the Io-controlled DAM.

From the dip angle plot in Figure 1 we see that Io crosses the dip equator at System III (1965) longitudes $\sim 115^{\circ}$ and 290°. This is close to the boundaries of the range of sub-Io longitudes for which we observe Io-controlled DAM. Apparently DAM is stimulated only when Io is north of the magnetic equator. That DAM is apparently beamed into the ecliptic only when Io is situated over an "active hemisphere" centered near 200° longitude was first pointed out by Dulk (1965).

III. The IFT Footprint

Figure 2 is a plot of the IFT foot print (i.e., the locus of foot points of the IFT for a complete rotation of the planet with respect to Io) in zenographic co-ordinates. For each point along the IFT foot print in the regions for which Io-controlled DAM is observed, we have plotted an arrow in a direction parallel to the corresponding central

meridian longitude for that DAM emission feature. If the Io-controlled emission originates from near the foot of the IFT then the four "source" regions would be at the indicated locations and the direction of emission in the ecliptic plane would be as given by the arrows. Note that the IFT foot point passes very close to the Northern magnetic pole as the IFT enters the "active hemisphere" and Io-controlled fourth and main source emission begin. If the DAM originates from the Northern IFT foot, then the source is confined to a relatively small zenographic area and the emission is beamed into a pattern that intersects the ecliptic in two directions separated by $\sim 150^{o}$. This was first suggested by Dulk in 1965 on the basis of his analysis of the Io control morphology.

IV. The IFT Geometry

We have also examined the magnetic field geometry for the IFT and results from that analysis are displayed in Figure 3. Starting with the vector orientation of the foot of the IFT in each hemisphere, we have calculated the angle between the field line at 1.0 R_J and an observer in the ecliptic as a function of Io phase and central meridian longitude. The IFT foot point is beyond the limb of the planet for the crossed-hatched areas of the diagram. Since a number of theories for the DAM emission mechanism favor radiation at right angles to the magnetic field, the loci of 90^{o} aspect angles are plotted for each hemisphere. The lightly shaded areas denote the regions of the Io

phase-central meridian longitude plane in which the four Io-controlled "sources" are observed.

In the North IFT foot point diagram in Figure 3, we find that the 90° aspect angle trace passes directly through the fourth and early source regions (Io phase of 80° - 110°, central meridian longitude of 40° - 180°). The observed high frequency limit of ~ 18 MHz for the fourth source is consistent with the finding that the IFT intersects the surface at a point beyond the limb for much of the fourth source longitude range. Hence, the low altitude, high gyrofrequency portion of the Northern IFT is obscured from view for fourth source geometries. The high longitude boundary of the early source at ~ 180° is apparently not a result of obscuration of the source region but a consequence of the Southward passage of Io across the magnetic equator, i.e. out of the "active hemisphere". The magnetic field geometry for the Southern foot of the IFT does not show any particular correspondence with the locations of the fourth and early sources.

The situation is less clear for the main and third sources (Io phase ~ 240°, central meridian longitude 220 - 360°). For the Northern foot of the IFT the aspect angle with respect to the magnetic field is ~ 60° for the main source and ~ 80° for the third source. In the Southern hemisphere these angles are ~ 100° and ~ 110° for the main and third sources, respectively. The main source region would be beyond the limb for Io-phase > 240° in the South, and the third source would be beyond the limb at all times if the North foot point is involved.

V Discussion

The observed DAM frequency range and the sense of frequency drift of the envelopes of the source dynamic spectra tend to favor the North foot point over the South as the more probable source location. For example, the observed drift from low to high frequency in the fourth source could be a result of changes in the degree to which the foot of the Northern IFT is occulted by the planetary disk with time. We have already noted that obscuration effects could explain the high frequency cut-off of the fourth source. The initial low to high frequency drift of early source dynamic spectra might also result from obscuration effects resulting from the close proximity of the North foot point of the IFT to the "horizon" for low values of Io phase and central meridian longitude in the early source portion of the diagram. The subsequent drift from high-to-low frequency in the later stages of many early source events could result from the high-to-low drift of the Northern IFT gyrofrequency with time as indicated in Figure 1. For the main and third sources the sense of variation of IFT gyrofrequency (high-to-low) matches the sense of observed frequency drift for main and third source dynamic spectra which is also from high-to-low frequency. The variation of gyrofrequency with sub-Io longitude in the Southern hemisphere does not agree with the observations as well. Limb obscuration effects in the North could contribute to the fact that the third source does not reach as high a frequency as either the main or early sources.

Although the discussion above has emphasized the positive aspects of a comparison of the Northern IFT geometry and DAM morphology, a number of difficulties remain to be resolved. For the range of sub-Io longitudes over which early source emission is observed, the IFT electron gyrofrequency never quite reaches the maximum observed DAM frequency ($\sim$ 34 MHz vs. 39.5 MHz). The predicted limb occultation of the North foot point for third source geometries plus the fact that the maximum IFT gyrofrequency in that region is only $\sim$ 28 MHz do not agree with the observed high frequency limit of $\sim$ 32 MHz for the third source if the emission is at the local gyrofrequency. With ionospheric electron densities of $\sim$ 3×10^5 cm^{-3} (Kliore et al., 1975) the upper hybrid resonance frequency will not be appreciably higher than the gyrofrequency. On the other hand, a radiation mechanism such as that discussed by Scarf (1973) where the radiation frequency is 3/2 times the gyrofrequency would not be similarly constrained by the magnetic field model. Furthermore, Kaiser and Alexander (1975) have recently shown that the terrestrial kilometric emission can apparently originate at heights well above the level at which the gyrofrequency equals the emission frequency. Perhaps the same processes can occur in Jupiter's magnetosphere.

VI. Conclusions

Taken as a whole, the comparison of Pioneer magnetic field models with the DAM morphology provides some encouraging lines of agreement,

but it falls short of leading to any fully satisfactory picture of the radio source. If our initial assumptions that the models portray the magnetic field topology near the surface reasonably accurately and that the Io flux tube determines the location of the source are correct, then simple free space geometric analyses do not suffice. We suspect that propagation effects are likely to play an important role in the DAM problem and that such effects will have to be considered in order to adequately account for the radio observations. For example, reflection of the radio waves off a surface such as the Jovian ionosphere may be responsible for the 90^{o} - 60^{o} asymetry in the aspect angles determined for the main and early sources. Similarly, propagation effects may be particularly important in determining the frequency structure of the dynamic spectra of the Io-controllled sources and in defining the radiation pattern of the emission. This is not a particularly new idea of course. The results of the Pioneer magnetic field measurements have just reinforced those conclusions.

Acknowledgements

We are indebted to our colleague N.F. Ness for his comments and suggestions during our many discussions on this work.

References

Acuña, M.H., and Ness, N.F., presented at Tucson Jupiter Workshop (May 1975); to appear in Jupiter, the Giant Planet, T. Gehrels ed. (Univ. of Arizona Press, 1976).

Dulk, G.A., Univ. of Colorado Ph.D. Thesis (1965).

Kaiser, M.L., and Alexander, J.K., USNC/URSI Annual Meeting, Boulder, Colorado (Oct. 1975).

Kliore, A., Fjeldbo, G., Seidel, B.L., Sesplaukis, T.T., Sweetnam, D.W., and Woiceshyn, P.M., Science 188, 474 (1975).

Riddle, A.C., presented at Tucson Jupiter Workshop (May 1975); to appear in Jupiter, The Giant Planet, T. Gehrels ed. (Univ. of Arizona Press, 1976).

Scarf, F.L., TRW Systems Rept. 24876-6001-RU-00 (1973)

Smith, E.J., Davis, L., Jones, D.E., Coleman, P.J., Colburn, D.S., Dyal, P., and Sonett, C.P., Science 188, 451 (1975).

Smith, R.A., and Wu, C.S., Astrophys. J. (Lett.) 190, L91 (1974). (Addendum: ibid 193, L101).

FIGURE CAPTIONS

Figure 1 (Lower panel) Plot of relative occurrence probability of DAM emission versus sub-Io System III (1965) longitude for the major Io-controlled sources. (Middle panel) Plot of magnetic dip angle at Io as a function of sub-Io longitude. (Top panel) Plot of the electron gyrofrequency at the feet of the Io flux tube as a function of sub-Io longitude.

Figure 2. Plot of the footprint of the Io flux tube as a function of System III (1965) longitude and zenographic latitude. The location of the magnetic pole at the surface for the Northern (left panel) and Southern (right panel) hemispheres is given by the upper case N and S respectively. The foot points are labelled to indicate the corresponding System III (1965) sub-Io longitude for each point. The arrows show the direction into which DAM emission is beamed if the major Io-controlled sources are located at the foot of the IFT.

Figure 3a. Angle between the North foot of the Io flux tube and an observer in the ecliptic ($D_E = 0^o$) as a function of Io phase and System III (1965) central meridian longitude. The hashed area denotes cases for which the foot point at the surface would be beyond the limb of the planet with respect to the observer. The dashed lines are the loci of 90^o aspect angle points. The shaded areas show the location of the major Io-controlled DAM emission regions.

3b. Same as 3a. but for the South foot of the Io flux tube.

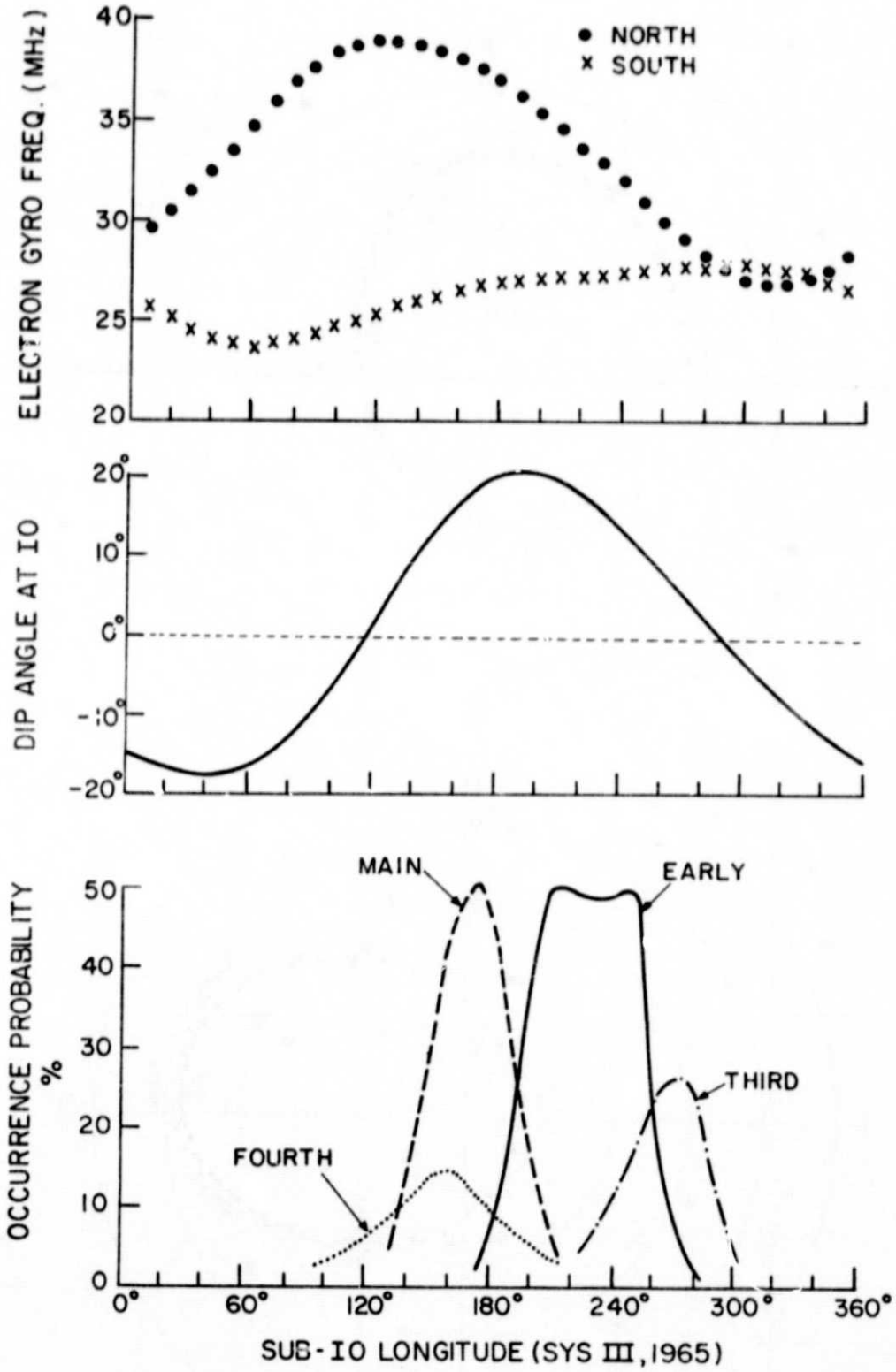
ELECTRON GYRO FREQ. (MHz)
40
35
30
25
20
NORTH
SOUTH
DIP ANGLE AT IO
20°
10°
0°
-10°
-20°
OCCURRENCE PROBABILITY
%
50
40
30
20
10
0
MAIN
EARLY
THIRD
FOURTH
0°
60°
120°
180°
240°
300°
360°
SUB-IO LONGITUDE (SYS III, 1965)

Figure 1

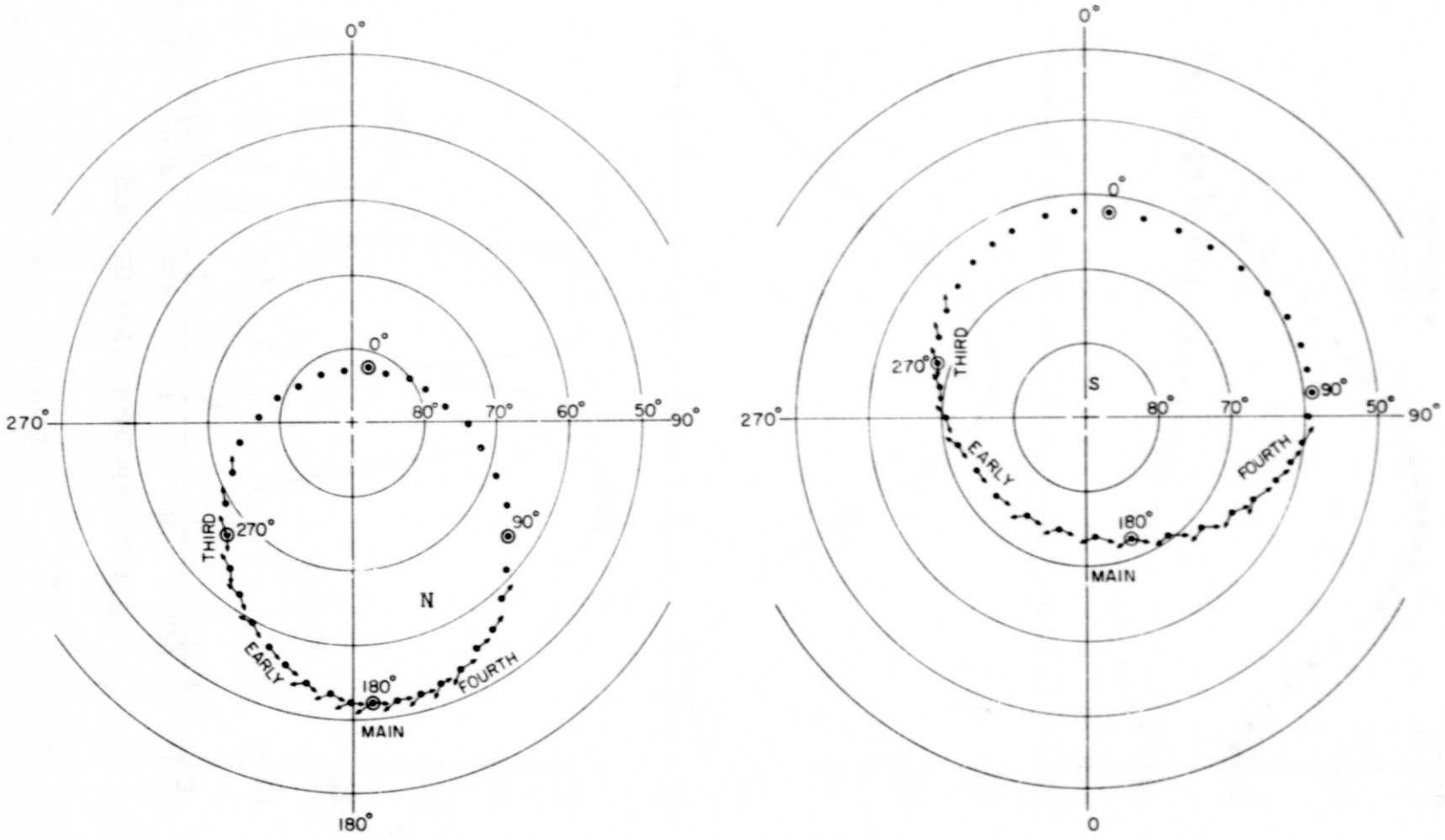

Figure 2

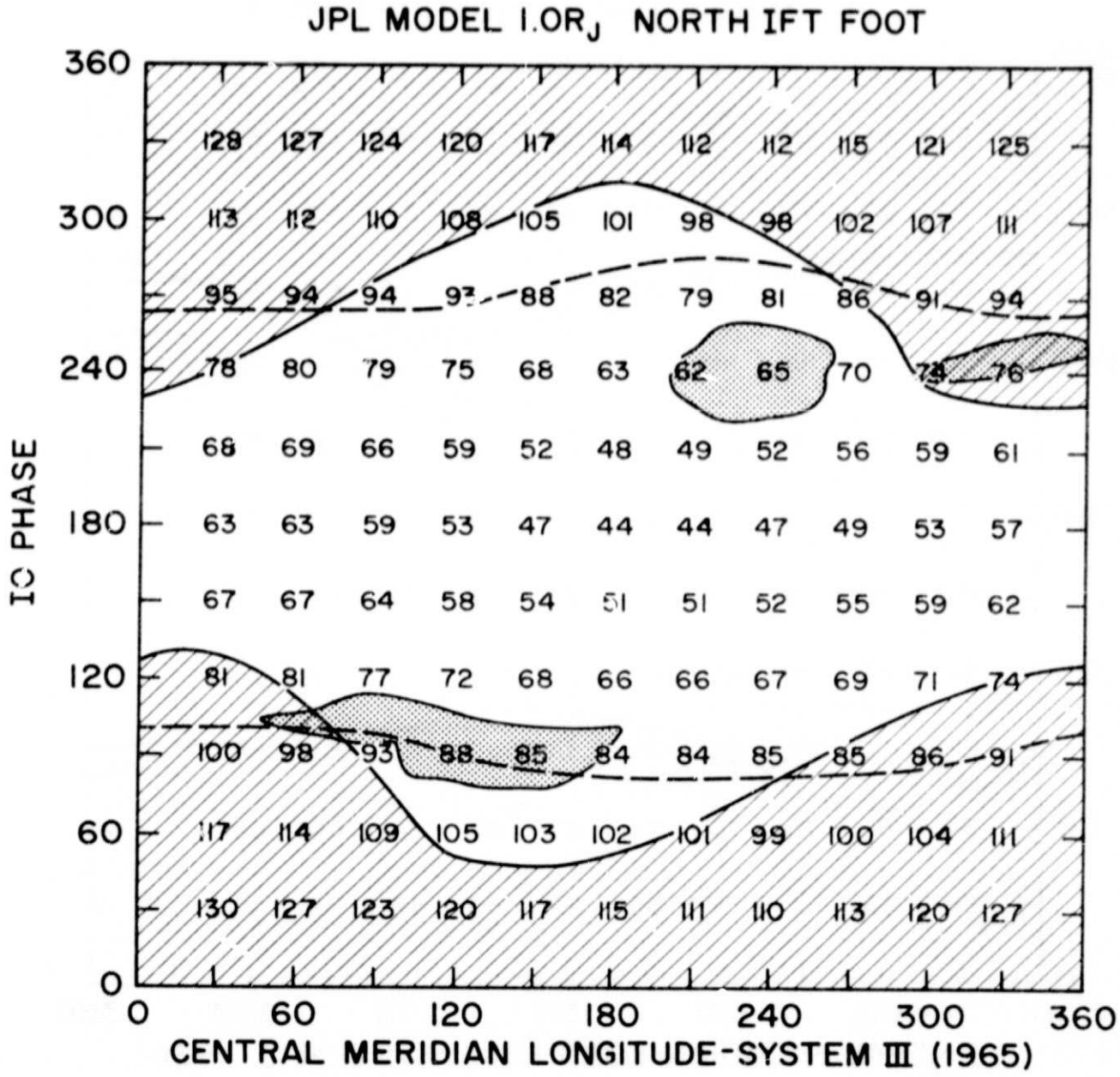
JPL MODEL I.OR$_J$ NORTH IFT FOOT
360
300
240
180
120
60
0
IO PHASE
128 127 124 120 117 114 112 112 115 121 125
113 112 110 108 105 101 98 98 102 107 111
95 94 94 93 88 82 79 81 86 91 94
78 80 79 75 68 63 62 65 70 74 76
68 69 66 59 52 48 49 52 56 59 61
63 63 59 53 47 44 44 47 49 53 57
67 67 64 58 54 51 51 52 55 59 62
81 81 77 72 68 66 66 67 69 71 74
100 98 93 88 85 84 84 85 85 86 91
117 114 109 105 103 102 101 99 100 104 111
130 127 123 120 117 115 111 110 113 120 127
0 60 120 180 240 300 360
CENTRAL MERIDIAN LONGITUDE-SYSTEM III (1965)

Figure 3a

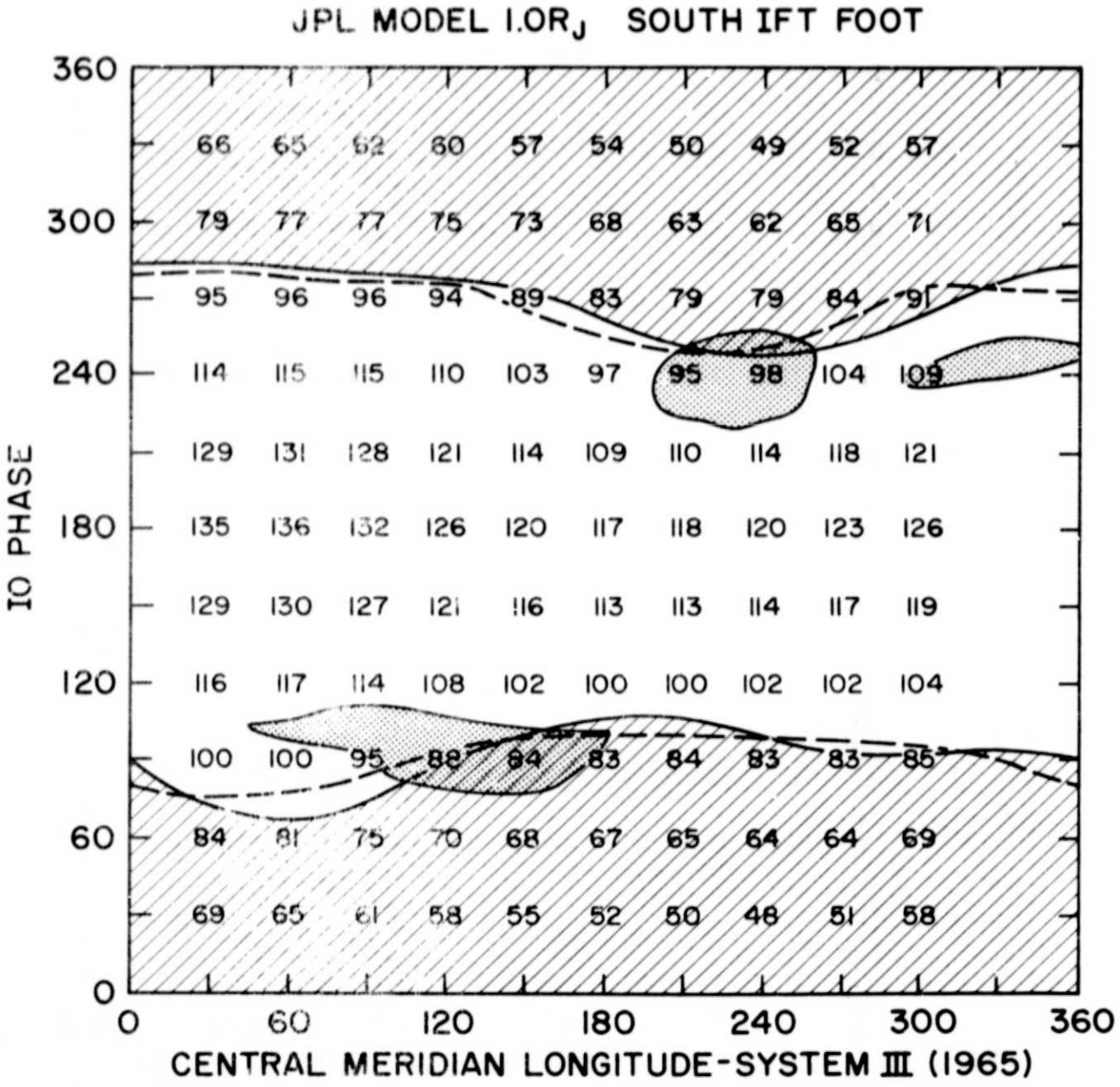
JPL MODEL I.OR$_J$ SOUTH IFT FOOT
IO PHASE
360
300
240
180
120
60
0
66 65 62 60 57 54 50 49 52 57
79 77 77 75 73 68 63 62 65 71
95 96 96 94 89 83 79 79 84 91
114 115 115 110 103 97 95 98 104 109
129 131 128 121 114 109 110 114 118 121
135 136 132 126 120 117 118 120 123 126
129 130 127 121 116 113 113 114 117 119
116 117 114 108 102 100 100 102 102 104
100 100 95 88 84 83 84 83 83 85
84 81 75 70 68 67 65 64 64 69
69 65 61 58 55 52 50 48 51 58
0 60 120 180 240 300 360
CENTRAL MERIDIAN LONGITUDE-SYSTEM III (1965)

Figure 3b